Predictions for supersymmetric particle masses using indirect experimental and cosmological constraints

O. Buchmueller,[a] **R. Cavanaugh,**[bc] **A. De Roeck,**[ad] **J.R. Ellis,**[a] **H. Flächer,**[a]
S. Heinemeyer,[e] **G. Isidori,**[fg] **K.A. Olive,**[h] **P. Paradisi,**[i] **F.J. Ronga**[j] **and G. Weiglein**[k]

[a] *CERN, CH-1211 Geneve 23, Switzerland*

[b] *Fermi National Accelerator Laboratory, P.O. Box 500, Batavia, Illinois 60510, U.S.A.*

[c] *Physics Department, University of Illinois at Chicago, Chicago, IL 60607-7059, U.S.A.*

[d] *Antwerp University, B-2610 Wilrijk, Belgium*

[e] *Instituto de Física de Cantabria (CSIC-UC), E-39005 Santander, Spain*

[f] *INFN, Laboratori Nazionali di Frascati, Via E. Fermi 40, I-00044 Frascati, Italy*

[g] *Scuola Normale Superiore, Piazza dei Cavalieri 7, I-56126 Pisa, Italy*

[h] *School of Physics and Astronomy, Univ. of Minnesota, Minneapolis, MN 55455, U.S.A.*

[i] *Physik-Department, Technische Universität München, D-85748 Garching, Germany*

[j] *Institute for Particle Physics, ETH Zürich, CH-8093 Zürich, Switzerland*

[k] *IPPP, University of Durham, Durham DH1 3LE, U.K.*

E-mail: `Oliver.Buchmuller@cern.ch`, `Richard.Cavanaugh@cern.ch`,
`deroeck@mail.cern.ch`, `John.Ellis@cern.ch`, `flaecher@mail.cern.ch`,
`Sven.Heinemeyer@cern.ch`, `Gino.Isidori@lnf.infn.it`, `OLIVE@physics.umn.edu`,
`Paride.Paradisi@uv.es`, `Frederic.Ronga@cern.ch`, `georg.weiglein@durham.ac.uk`

ABSTRACT: In view of the imminent start of the LHC experimental programme, we use the available indirect experimental and cosmological information to estimate the likely range of parameters of the constrained minimal supersymmetric extension of the Standard Model (CMSSM), using a Markov-chain Monte Carlo (MCMC) technique to sample the parameter space. The 95% confidence-level area in the $(m_0, m_{1/2})$ plane of the CMSSM lies largely within the region that could be explored with $1 \, \text{fb}^{-1}$ of integrated luminosity at $14 \, \text{TeV}$, and much of the 68% confidence-level area lies within the region that could be explored with $50 \, \text{pb}^{-1}$ of integrated luminosity at $10 \, \text{TeV}$. A same-sign dilepton signal could well be visible in most of the 68% confidence-level area with $1 \, \text{fb}^{-1}$ of integrated luminosity at $14 \, \text{TeV}$. We discuss the sensitivities of the preferred ranges to variations in the most relevant indirect experimental and cosmological constraints and also to deviations from the universality of the supersymmetry-breaking contributions to the masses of the Higgs bosons.

Contents

1. Introduction

Supersymmetry (SUSY) [1–3] is one of the most highly favoured extensions of the Standard Model (SM), and is often considered to be a prime candidate for discovery at the Large Hadron Collider (LHC). With the start of experiments at the LHC now becoming imminent, it is natural and topical to make the best possible assessment of the likelihood that the LHC will indeed discover SUSY, based on the best available experimental, phenomenological and cosmological information. Most of the current constraints on possible physics beyond the SM are negative, in the sense that they reflect the agreement of data with the SM, and set only lower limits on the possible masses of supersymmetric particles [4]. Examples are direct constraints such as lower limits on specific sparticles, e.g., the chargino, and indirect constraints such as the lower limit on the possible mass of a SM-like Higgs boson [5, 6].

However, there are two observational constraints that, within the context of SUSY, may be used also to set upper limits on the possible masses of supersymmetric particles, since they correspond to measurements that cannot be explained by the SM alone. These hints for new physics are the anomalous magnetic moment of the muon, $(g-2)_\mu$, which appears to differ by over three standard deviations from the best SM calculation based on low-energy e^+e^- data [7–13], and the density of cold dark matter, Ω_{CDM} [14], which has no possible origin within the SM. Each of these discrepancies has many possible interpretations, of which SUSY is just one. Nevertheless, given the strong motivations for SUSY, which include the naturalness of the mass hierarchy and grand unification, as well as the existence of a plausible candidate for the astrophysical cold dark matter, it is natural to ask what $(g-2)_\mu$ and Ω_{CDM} may imply for the parameters of supersymmetric models. Any such analysis should also take into account the constraints imposed by precision measurements of electroweak observables (EWPO) and B-physics observables (BPO) such as BR($b \to s\gamma$), where most observables agree quite well with the SM.

– 1 –

In this paper we revisit the indirect information on supersymmetric model parameters obtainable in the light of these experimental, phenomenological and cosmological constraints, using a Markov-chain Monte Carlo (MCMC) approach, see, e.g., ref. [15] and references therein. This is practical only in simplified versions of the minimal supersymmetric extension of the Standard Model (MSSM), in which some universality relations are imposed on the soft SUSY-breaking parameters. Initially, we work in the framework of the constrained MSSM (CMSSM), in which the scalar and gaugino mass parameters, m_0, $m_{1/2}$, and the trilinear coupling A_0 are each assumed to be equal at the input GUT scale. Furthermore as low-energy parameter we have $\tan\beta$, the ratio of the two vacuum expectation values of the two Higgs doublets. At the end we also comment on the possible changes in our results if the common soft SUSY-breaking contribution to the Higgs scalar masses-squared, m_H^2, is allowed to differ from those of the squarks and sleptons, the single-parameter non-universal Higgs model or NUHM1.

There have been many previous studies of the CMSSM parameter space [16–48], including estimates of the sparticle masses, and a number of these have used MCMC techniques [34–43]. These have been used to extract the preferred values for the CMSSM parameters using low-energy precision data, bounds from astrophysical observables and flavour-related observables. These analyses differ in the precision observables that have been considered, the level of sophistication of the theory predictions that have been used, and the way the statistical analysis has been performed.

Here we use the MCMC technique to sample efficiently the SUSY parameter space, and thereby construct the χ^2 probability function, $P(\chi^2, N_{\mathrm{dof}})$. This accounts correctly for the number of degrees of freedom, N_{dof}, and thus represents a quantitative measure for the quality-of-fit. Hence $P(\chi^2, N_{\mathrm{dof}})$ can be used to estimate the absolute probability with which the CMSSM describes the experimental data. Our probabilistic treatment is explained in detail in section 2.

Many previous analyses found evidence for a relatively low SUSY mass scale in the stau-coannihilation region, e.g., [32, 47, 49], and a mild preference for $\tan\beta \sim 10$ was found in [47]. A comparison of Bayesian analyses yielding varying results under different assumptions was made in [48]. Some differences between analyses may also be traceable to the treatments of the BR($b \to s\gamma$) and $(g-2)_\mu$ measurements, which we discuss in some detail below.

Our main objectives in this paper are threefold. One is to discuss explicitly the prospects for discovering sparticles in early LHC running, another is to discuss the robustness of the fit results by analyzing the implications of relaxing the constraints due to $(g-2)_\mu$, BR($b \to s\gamma$), Ω_{CDM} and other observables, and the third is to discuss the extension of the CMSSM results to the NUHM1, in which an extra parameter is introduced that allows a common degree of non-universality for the two Higgs multiplets.

We find that the 95% C.L. area in the $(m_{1/2}, m_0)$ plane of the CMSSM lies largely within the region that could be explored with $1\,\mathrm{fb}^{-1}$ of integrated LHC luminosity at $14\,\mathrm{TeV}$ in a single experiment, and that much of the 68% C.L. area lies within the region that could be explored with $50\,\mathrm{pb}^{-1}$ of integrated luminosity at $10\,\mathrm{TeV}$ (the projected initial LHC collision energy). A same-sign dilepton signal could well be visible in the

68% C.L. area with $1\,\mathrm{fb}^{-1}$ of integrated luminosity at $14\,\mathrm{TeV}$, and the lightest Higgs boson might also be detectable in squark decays with $2\,\mathrm{fb}^{-1}$ of integrated luminosity at $14\,\mathrm{TeV}$. We find that removing the Ω_{CDM} constraint has little effect on the preferred regions of the CMSSM parameter space in the $(m_0, m_{1/2})$, $(\tan\beta, m_{1/2})$, and $(\tan\beta, m_0)$ planes, apart from expanding the range of m_0, particularly for $\tan\beta \sim 10$. On the other hand, rescaling the present error in $(g-2)_\mu$ may have quite an important effect: the preferred ranges in $m_{1/2}$ and m_0 would expand quite significantly if the error on the present experimental discrepancy with the SM were to be increased. Conversely, if this error could be reduced, e.g., by a more precise measurement of $(g-2)_\mu$ and/or a more refined theoretical estimate within the SM, the predictions for sparticle masses could be significantly improved. We also discuss the effects of possible variations in the errors in $\mathrm{BR}(b \to s\gamma)$ and other observables. Finally, we show that our results would not be greatly changed in the NUHM1: we leave a more complete study of the NUHM1 and the NUHM2 (in which the masses of the two Higgs multiplets are independently non-universal) for future work.

2. Multi-parameter fit to experimental observables

Important observables used in our analysis are listed in table 1. Some of the EWPO that are included in the analysis have not been listed in the table, because they did not change since the analysis carried out in [47]; their details can be found there.

The deviation of $(g-2)_\mu$ from the SM prediction by more than $3\,\sigma$ can be easily accommodated within the (C)MSSM by choosing appropriately the sign of the Higgs supermultiplet mixing parameter, μ: $\mathrm{sign}(\mu) = \mathrm{sign}(a_\mu^{\mathrm{exp}} - a_\mu^{\mathrm{SM}})$. Consequently, we analyze in detail the case $\mu > 0$, and discuss the $\mu < 0$ case only briefly.

The central value of the $\mathrm{BR}(b \to s\gamma)$ constraint has changed slightly because of new experimental results: the data/SM ratio in table 1 corresponds to the HFAG average $\mathrm{BR}(b \to s\gamma) = (3.52 \pm 0.24) \times 10^{-5}$ [66] and to the NNLO SM calculation, $\mathrm{BR}(b \to s\gamma) = (3.15 \pm 0.23) \times 10^{-5}$ [61] (both values refer to the inclusive rate with $E_\gamma > 1.6\,\mathrm{GeV}$). Despite some interesting recent attempts to improve the SM prediction of $\mathrm{BR}(b \to s\gamma)$ (see, e.g., refs. [85–88] and references therein), following ref. [88] we still consider the above NNLO value as the most reliable SM estimate. As compared to [47], we have reduced the additional theoretical error in the calculation of the SUSY contribution, for the following reasons. First, it should be noted that all non-perturbative uncertainties cancel out in the SUSY/SM ratio. Secondly, data force the deviations from the SM to be small in $\mathrm{BR}(b \to s\gamma)$, so the SUSY/SM ratio can be computed to a relatively high degree of accuracy.[1] A conservative 15% error on the $b \to s\gamma$ SUSY amplitude corresponds to less than 5% in the $\mathrm{BR}_{\mathrm{b}\to\mathrm{s}\gamma}^{\mathrm{SUSY}}/\mathrm{BR}_{\mathrm{b}\to\mathrm{s}\gamma}^{\mathrm{SM}}$ ratio in the region where this does not deviate from

---

[1]There are two exceptional cases where the theoretical uncertainties of the SUSY amplitude can be large: i) the SUSY amplitude is about twice the SM one (SUSY/SM~ -2) yielding a $\mathrm{BR}(b \to s\gamma)$ rate close to the SM value ii) the overall SUSY contribution is small because of cancellations among independent large terms. Case i) is excluded by the $B \to X_s \ell^+\ell^-$ constraints [89, 90] that we take into account in our numerical analysis. We deal with case ii) by implementing in our code the leading NLO SUSY contributions, that are known within the MFV framework [91, 62].

Observable	Th. Source	Ex. Source	Constraint	Add. Th. Unc.
$m_W\,[\mathrm{GeV}]$	[50, 51]	[52]	80.399 ± 0.025	0.010
$a_\mu^{\mathrm{exp}} - a_\mu^{\mathrm{SM}}$	[8, 53–55]	[7, 10, 56]	$(30.2 \pm 8.8) \times 10^{-10}$	2.0×10^{-10}
$m_h\,[\mathrm{GeV}]$	[57–60]	[5, 6]	> 114.4 (see text)	3.0
$\mathrm{BR}_{\mathrm{b}\to\mathrm{s}\gamma}^{\mathrm{exp}}/\mathrm{BR}_{\mathrm{b}\to\mathrm{s}\gamma}^{\mathrm{SM}}$	[61–65]	[66]	$1.117 \pm 0.076_{\mathrm{exp}} \pm 0.082_{\mathrm{th(SM)}}$	0.050
$m_t\,[\mathrm{GeV}]$	[50, 51]	[67]	172.4 ± 1.2	—
$\Omega_{\mathrm{CDM}}h^2$	[68–70]	[14]	0.1099 ± 0.0062	0.012
$\mathrm{BR}(B_s \to \mu^+\mu^-)$	[71–74]	[66]	$< 4.7 \times 10^{-8}$	0.02×10^{-8}
$\mathrm{BR}_{\mathrm{B}\to\tau\nu}^{\mathrm{exp}}/\mathrm{BR}_{\mathrm{B}\to\tau\nu}^{\mathrm{SM}}$	[73–75]	[76–78]	$1.15 \pm 0.40_{\mathrm{[exp+th]}}$	—
$\mathrm{BR}(B_d \to \mu^+\mu^-)$	[71–74]	[66]	$< 2.3 \times 10^{-8}$	0.01×10^{-9}
$\mathrm{BR}_{B\to X_s\ell\ell}^{\mathrm{exp}}/\mathrm{BR}_{B\to X_s\ell\ell}^{\mathrm{SM}}$	[79]	[66, 80]	0.99 ± 0.32	—
$\mathrm{BR}_{K\to\mu\nu}^{\mathrm{exp}}/\mathrm{BR}_{K\to\mu\nu}^{\mathrm{SM}}$	[73, 75]	[81]	$1.008 \pm 0.014_{\mathrm{[exp+th]}}$	—
$\mathrm{BR}_{K\to\pi\nu\bar\nu}^{\mathrm{exp}}/\mathrm{BR}_{K\to\pi\nu\bar\nu}^{\mathrm{SM}}$	[82]	[83]	< 4.5	—
$\Delta M_{B_s}^{\mathrm{exp}}/\Delta M_{B_s}^{\mathrm{SM}}$	[82]	[84]	$1.11 \pm 0.01_{\mathrm{exp}} \pm 0.32_{\mathrm{th(SM)}}$	—
$\dfrac{(\Delta M_{B_s}^{\mathrm{exp}}/\Delta M_{B_s}^{\mathrm{SM}})}{(\Delta M_{B_d}^{\mathrm{exp}}/\Delta M_{B_d}^{\mathrm{SM}})}$	[71–74]	[66, 84]	$1.09 \pm 0.01_{\mathrm{exp}} \pm 0.16_{\mathrm{th(SM)}}$	—
$\Delta\epsilon_K^{\mathrm{exp}}/\Delta\epsilon_K^{\mathrm{SM}}$	[82]	[84]	$0.92 \pm 0.14_{\mathrm{[exp+th]}}$	—

Table 1: List of experimental constraints used in this work in addition to the electroweak observables listed in [47]. The top part of the table shows observables that are very sensitive to the MSSM parameter space, the middle part lists observables with updated measurements compared to [47] while the bottom part lists additional experimental constraints. The values and errors shown are the current best understanding of these constraints. The rightmost column displays additional theoretical uncertainties taken into account when implementing these constraints in the MSSM.

unity by more than 30%. The $\mathrm{BR}(b \to s\gamma)$ constraint, as well as all the other flavour-physics constraints listed in table 1, have been implemented using the code developed in refs. [73, 74]. This includes the leading NLO QCD corrections to the supersymmetric contributions [62] and a complete resummation of all the relevant large $\tan\beta$ effects beyond the lowest order [63–65]. More recent public codes for the evaluation of $\mathrm{BR}(b \to s\gamma)$ in the CMSSM have been presented in ref. [92, 93].

A significant B-physics constraint arises also from $\mathrm{BR}(B \to \tau\nu)$, which represents a powerful probe of the $(m_{H^\pm}, \tan\beta)$ plane [73, 74]. However, at present both experimental and theoretical uncertainties prevent us from fully exploiting the potential sensitivity of this observable. In particular, the SM prediction suffers from the uncertainties in the determination of the CKM element $|V_{\mathrm{ub}}|$ and of the decay constant f_B. Concerning $|V_{\mathrm{ub}}|$, we use the current HFAG average [66] (from combined exclusive and inclusive semileptonic B decays), while for f_B we use the lattice result of [78]. An alternative way to reduce the theoretical error associated to $\mathrm{BR}(B \to \tau\nu)_{\mathrm{SM}}$ is to consider the ratio $\mathrm{BR}(B \to \tau\nu)/\Delta M_{B_d}$, where f_B drops out and $|V_{\mathrm{ub}}|$ is replaced by $|V_{\mathrm{ub}}/V_{\mathrm{td}}| = \sin\beta/\sin\gamma$ [73, 74]. However, as the experimental error on $\mathrm{BR}(B \to \tau\nu)$ is the dominant uncertainty, this alternative

way does not lead to a significant reduction in the error. Moreover, it complicates the analysis since BR(B → τν) and ΔM_{B_d} are affected by independent SUSY contributions. For these reasons, we treat the two constraints separately. More precisely, we treat separately BR(B → τν), ΔM_{B_s}, and the ratio $\Delta M_{B_d}/\Delta M_{B_s}$. Similarly to BR(b → sγ), all flavour-physics constraints apart from BR($B_{s,d} → \mu^+\mu^-$) are implemented normalising the observables to the corresponding SM values.

The direct experimental limit on the Higgs-boson mass in the SM obtained at LEP [5] is $m_h > 114.4$ GeV at the 95% C.L. The corresponding bound within the MSSM could in principle be substantially lower, due to a reduced ZZh coupling or due to different, more complicated decay modes of the Higgs bosons [6]. However, it has been shown [94, 95] that these mechanisms cannot be realised within the CMSSM, and hence the experimental lower bound of 114.4 GeV can be applied.[2] For our fit we use the full likelihood information of the exclusion bound, given by the $CL_s(m_h)$ value, which is convoluted with a theory error on the evaluation of m_h of 3 GeV [57], according to the detailed prescription found in [29].

The numerical evaluation has been performed with the `MasterCode` that consistently combines the codes responsible for RGE running, for which we use `SoftSUSY` [96], and the various low-energy observables. At the electroweak scale we have included the following codes: `FeynHiggs` [57 – 60] for the evaluation of the Higgs masses and a_μ^{SUSY}; a code based on [73, 74] and `SuperIso` [93] for the flavour observables; a code based on [50, 51] for the electroweak precision observables; `MicrOMEGAs` [68 – 70] and `DarkSUSY` [97, 98] for the observables related to dark matter. We made extensive use of the SUSY Les Houches Accord [99] in the combination of the various codes within the `MasterCode`.

The CMSSM parameter space has been sampled using the MCMC technique. We treat $m_{1/2}$, m_0, A_0 and $\tan\beta$ as free parameters, and the Higgs mixing parameter μ and the pseudoscalar Higgs mass m_A as dependent parameters determined by the electroweak vacuum conditions.

A global χ^2 function is defined, which combines all calculations with experimental constraints:

$$\chi^2 = \sum_i^N \frac{(C_i - P_i)^2}{\sigma(C_i)^2 + \sigma(P_i)^2} + \sum_i \frac{(f_{\text{SM}_i}^{\text{obs}} - f_{\text{SM}_i}^{\text{fit}})^2}{\sigma(f_{\text{SM}_i})^2} \tag{2.1}$$

Here N is the number of observables studied, C_i represents an experimentally measured value (constraint) and each P_i defines a CMSSM parameter-dependent prediction for the corresponding constraint. The three SM parameters $f_{\text{SM}} = \{\Delta\alpha_{\text{had}}, m_t, m_Z\}$ are included as fit parameters and constrained to be within their current experimental resolution $\sigma(f_{\text{SM}})$.

As indicated in section 1, the sensitivity of the global fit to different constraint scenarios is studied below by removing the Ω_{CDM} constraint or rescaling the $(g-2)_\mu$ and other experimental uncertainties. Since each new scenario represents a new χ^2 function which must be minimized, multiple re-samplings of the full multi-dimensional parameter space are, in principle, required to determine the most probable fit regions for each scenario and would be computationally too expensive.

---

[2]Following ref. [32], for simplicity we use this bound also in our NUHM1 analysis. As discussed below, the best-fit NUHM1 point we find yields m_h well above this bound.

To avoid this difficulty, we analyze the effect of removing the $\Omega_{\rm CDM}$ constraint by exploiting the fact that independent χ^2 functions are additive and result in a well-defined χ^2 probability. Hence, a "loose" χ^2 function, $\chi^2_{\rm loose}$, is defined in which the term representing the $\Omega_{\rm CDM}$ constraint is removed from the original χ^2. The $\chi^2_{\rm loose}$ function represents the likelihood that a particular set of model parameter values is compatible with a sub-set of the experimental data constraints, without any experimental knowledge of $\Omega_{\rm CDM}$.

An exhaustive, and computationally expensive, 25 million point pre-sampling of the $\chi^2_{\rm loose}$ function in the full multi-dimensional model parameter space is then performed using an MCMC. The result of this pre-sampling identifies fit regions which are generally excluded by the considered sub-set of experimental data. Any regions excluded by the less constrained fit will also be excluded with the inclusion of additional experimental constraints and, in particular, with different scenarios for the $\Omega_{\rm CDM}$ constraint. Hence, without loss of generality, this pre-sampling procedure reduces the hyper-volume of parameter space which needs to be searched multiple times over in the context of different constraint scenarios to a computationally manageable level.

Constraint terms representing the different $\Omega_{\rm CDM}$ scenarios are then re-instated to form different $\chi^2 = \chi^2_{\rm loose} + \chi^2_{\rm scenario}$ functions, one for each scenario studied. The precise values of the most probable fit parameters are determined via a full MINUIT [100] minimization of the χ^2 for each different scenario, but are performed only within the general parameter space regions not already excluded from the pre-sampling of the $\chi^2_{\rm loose}$ function. An MCMC final sampling is subsequently used to determine the 68% and 95% likelihood contours for each scenario constraint studied.

Additionally, later on we vary the uncertainties of $\Omega_{\rm CDM}$ and other constraints using similar techniques. This allows us to study and compare the effects of such variations on the χ^2 fit and the most probable parameters.

3. Results

3.1 Predictions for LHC discoveries

In figure 1 we display the best-fit value and the 68% and 95% likelihood contours for the CMSSM $(m_0, m_{1/2})$ plane, obtained as described in section 2 from a fit taking into account all experimental constraints listed in table 1 as well as the constraints from the additional electroweak observables listed in [47]. We also show in the upper panel of figure 1 various LHC sparticle discovery contours for $1\,{\rm fb}^{-1}$ of good-quality data in a single experiment at a centre-of-mass energy of 14 TeV. The ATLAS and CMS collaborations have each published 5-σ discovery contours in the CMSSM $(m_{1/2}, m_0)$ plane for $A_0 = 0$ and $\tan\beta = 10$ [101 – 103]. Their contours are generally very similar, and the solid brown contour displayed is that published by CMS for the most sensitive jets + missing E_T search. This contour is insensitive to A_0, which affects primarily the third-generation sparticle masses, since the main discovery channels involve gluinos and first-generation squarks. The discovery contours are also not very sensitive to $\tan\beta$, since the gluino mass is insensitive to this variable, and the first-generation squark masses are also not very sensitive to $\tan\beta$. Therefore, it is a reasonable first approximation to compare our 68%
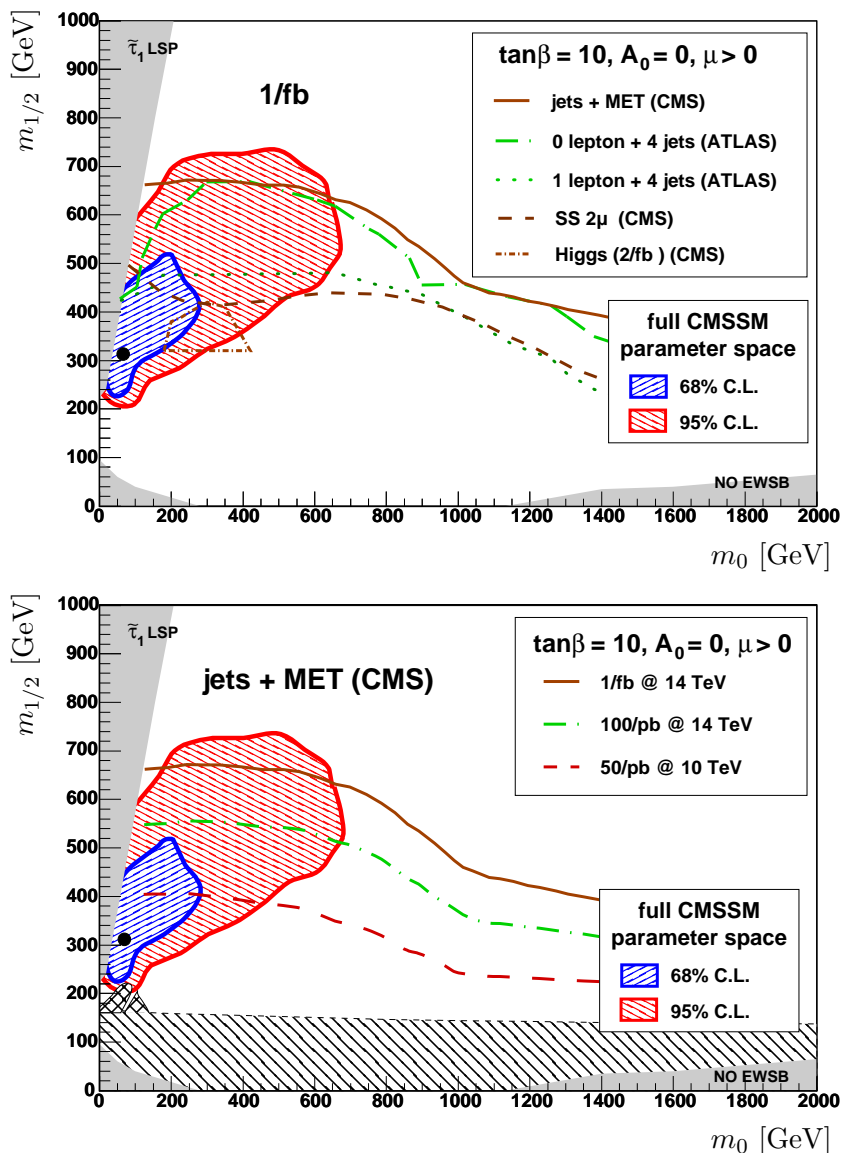
Figure 1: The $(m_0, m_{1/2})$ plane in the CMSSM for $\tan\beta = 10$ and $A_0 = 0$. The dark shaded area at low m_0 and high $m_{1/2}$ is excluded due to a scalar tau LSP, the light shaded areas at low $m_{1/2}$ do not exhibit electroweak symmetry breaking. The nearly horizontal line at $m_{1/2} \approx 160\,\mathrm{GeV}$ in the lower panel has $m_{\tilde{\chi}_1^\pm} = 103\,\mathrm{GeV}$, and the area below is excluded by LEP searches. Just above this contour at low m_0 in the lower panel is the region that is excluded by trilepton searches at the Tevatron. Shown in both plots are the best-fit point, indicated by a filled circle, and the 68 (95)% C.L. contours from our fit as dark grey/blue (light grey/red) overlays, scanned over all $\tan\beta$ and A_0 values. Upper plot: Some $5\,\sigma$ discovery contours at ATLAS and CMS with $1\,\mathrm{fb}^{-1}$ at 14 TeV, and the contour for the $5\,\sigma$ discovery of the Higgs boson in sparticle decays with $2\,\mathrm{fb}^{-1}$ at 14 TeV in CMS. Lower plot: The $5\,\sigma$ discovery contours for jet + missing E_T events at CMS with $1\,\mathrm{fb}^{-1}$ at 14 TeV, 100 pb^{-1} at 14 TeV and 50 pb^{-1} at 10 TeV centre-of-mass energy.

and 95% likelihood contours directly with the discovery contours given for $A_0 = 0$ and $\tan\beta = 10$ fixed, particularly since the best fit has a similar value of $\tan\beta$.

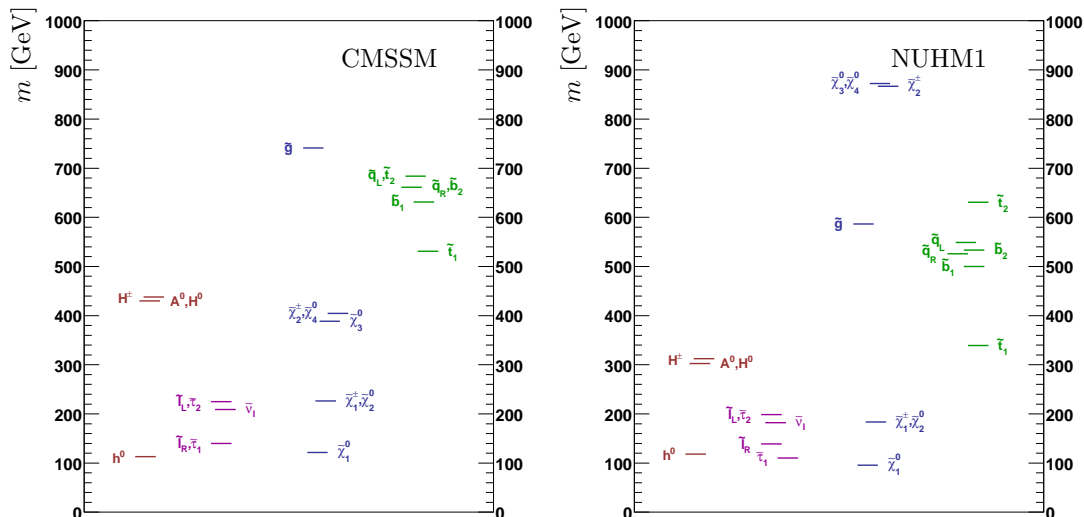The parameters of the best-fit CMSSM point are $m_{1/2} = 310\,\mathrm{GeV}$, $m_0 = 60\,\mathrm{GeV}$,

Figure 2: The spectra at the best-fit points: left — in the CMSSM with $m_0 = 60\,\mathrm{GeV}$, $m_{1/2} = 310\,\mathrm{GeV}$, $A_0 = 240\,\mathrm{GeV}$, $\tan\beta = 11$, and right — in the NUHM1 with $m_0 = 100\,\mathrm{GeV}$, $m_{1/2} = 240\,\mathrm{GeV}$, $A_0 = -930\,\mathrm{GeV}$, $\tan\beta = 7$, $m_H^2 = -6.9 \times 10^5\,\mathrm{GeV}^2$ and $\mu = 870\,\mathrm{GeV}$.

$A_0 = 240\,\mathrm{GeV}$, $\tan\beta = 11$ and $\mu = 380\,\mathrm{GeV}$,[3] yielding the overall $\chi^2/\mathrm{N_{dof}} = 20.4/19$ (37.3% probability) and $m_h = 113.2\,\mathrm{GeV}$.[4] The overall value of the χ^2 at the minimum is somewhat pushed up by the value of m_h, which is uncomfortably low. However, it is acceptable within the higher-order calculational uncertainties expected in the `FeynHiggs` code that we use here, $\delta m_h^{\mathrm{theo}} \approx 3\,\mathrm{GeV}$ [57]. As we discuss below, this slight tension is removed in the NUHM1 model, which correspondingly has a somewhat lower overall χ^2 (yielding a similar fit probability for the two models). The spectrum at the best-fit CMSSM point is shown in the left panel of figure 2. It is interesting to note that the best-fit CMSSM point and the corresponding spectrum are quite similar to the well-known SPS1a benchmark point [104], whose phenomenology at future colliders has been studied in considerable detail (see, e.g., [105 – 107]).

Comparing the 95% likelihood contour provided by the multi-parameter fit with the $1\,\mathrm{fb}^{-1}$ LHC discovery contour, we see that the former is almost entirely contained within the latter, implying that, if the CMSSM were correct, the LHC would be almost 'guaranteed', with 95% confidence, to discover SUSY with $1\,\mathrm{fb}^{-1}$ of good-quality data at 14 TeV. We also display in the upper panel of figure 1 contours representing the $5\,\sigma$ discovery reach with $1\,\mathrm{fb}^{-1}$ at 14 TeV for 4-jet events with and without a charged lepton, for same-sign dilep-tons [102], denoted by SS, and (with $2\,\mathrm{fb}^{-1}$) for the lightest MSSM Higgs boson produced in cascade decays of sparticles [102], denoted by h. We see that the same-sign dilepton discovery region largely covers the 68% likelihood region of the CMSSM $(m_0, m_{1/2})$ plane. Thus, this signature could serve as a clean signal capable of confirming the supersymmetric interpretation of any jets + missing E_T signal observed in initial LHC running. On the

---

[3]Here and later, we quote CMSSM and NUHM1 input mass parameters with 10 GeV accuracy.

[4]The CMSSM fit quality has improved relative to [47] primarily because of the new value of m_t and the inclusion of more observables, that are generally highly consistent with the CMSSM.

other hand, the region where the lightest Higgs boson could be discovered in cascade decays of squarks with $2\,\mathrm{fb}^{-1}$ at $14\,\mathrm{TeV}$ lies largely between the 95% and 68% C.L. contours.

We have used PROSPINO2 [108] to estimate the variation of the discovery reach of the LHC jets + missing E_T search as a function of the integrated luminosity and the centre-of-mass energy. We display in the lower panel of figure 1 (green) dot-dashed and (red) dashed contours representing, respectively, the discovery reaches expected with $100\,\mathrm{pb}^{-1}$ at $14\,\mathrm{TeV}$ and $50\,\mathrm{pb}^{-1}$ at $10\,\mathrm{TeV}$. We see that the 68% likelihood contour is well covered by the $14\,\mathrm{TeV}/100\,\mathrm{pb}^{-1}$ discovery reach, and even the $10\,\mathrm{TeV}/50\,\mathrm{pb}^{-1}$ reach would be sufficient to discover SUSY at the best-fit point, indicated by a filled circle in figure 1. The lower panel of figure 1 also displays the regions of the CMSSM $(m_0, m_{1/2})$ plane that are excluded by chargino searches at LEP and by sparticle searches at the Tevatron [4, 109, 110]. The region excluded by the LEP Higgs search is sensitive to $\tan\beta$ and A_0, is subject to theoretical uncertainties, and, moreover, the experimental Higgs likelihood function is not a simple step function. Hence, it is not shown in figure 1.[5]

3.2 Sensitivity to experimental constraints

The above analysis assumed the default implementations of the experimental, phenomenological and cosmological constraints discussed in the previous section. We now discuss the possible effects of relaxing (or strengthening) some of the key constraints, starting with the relic cold dark matter density, Ω_{CDM}.

It is well-known that this constraint essentially reduces the dimensionality of the MSSM parameter space by one unit, fixing one combination of the parameters with an accuracy of a few %. For example, in the CMSSM for any pair of fixed values of A_0 and $\tan\beta$, the Ω_{CDM} constraint largely determines m_0 as a function of $m_{1/2}$, except for a discrete ambiguity associated with the coannihilation strip, the focus-point strip and the rapid-annihilation funnel that appears at large $\tan\beta$. Therefore, one might expect that dropping the Ω_{CDM} constraint would have a strong effect on the preferred region of the CMSSM $(m_{1/2}, m_0)$ plane shown in figure 1.

There are various possible reasons why one might consider dropping the dark matter constraint. Perhaps the neutralino is not the LSP? Perhaps R-parity is not quite conserved? Perhaps the early thermal history of the Universe differed from that usually assumed when calculating the relic LSP density? Perhaps Nature is described by some generalization of the CMSSM such as a model with non-universal SUSY-breaking contributions to the Higgs scalar masses (NUHM), in which case values of m_0 very different from those in the CMSSM might be permitted?

We show in figure 3 the effect of dropping the Ω_{CDM} constraint. This is significant in the upper panels, which display the $(m_0, m_{1/2})$ and $(\tan\beta, m_0)$ planes, but is not so important in the $(\tan\beta, m_{1/2})$ and $(A_0, m_{1/2})$ planes shown in the two lower panels of figure 3. These behaviours can be understood by recalling the behaviour of the WMAP coannihilation strips in the CMSSM $(m_{1/2}, m_0)$ planes for different values of $\tan\beta$. For

---

[5]However, for orientation, we note that if $m_0 = 0$, $\tan\beta = 10$ and $A_0 = 0$ the evaluation with FeynHiggs yields a nominal value of $m_h = 114.4\,\mathrm{GeV}$ for $m_{1/2} = 307\,\mathrm{GeV}$.
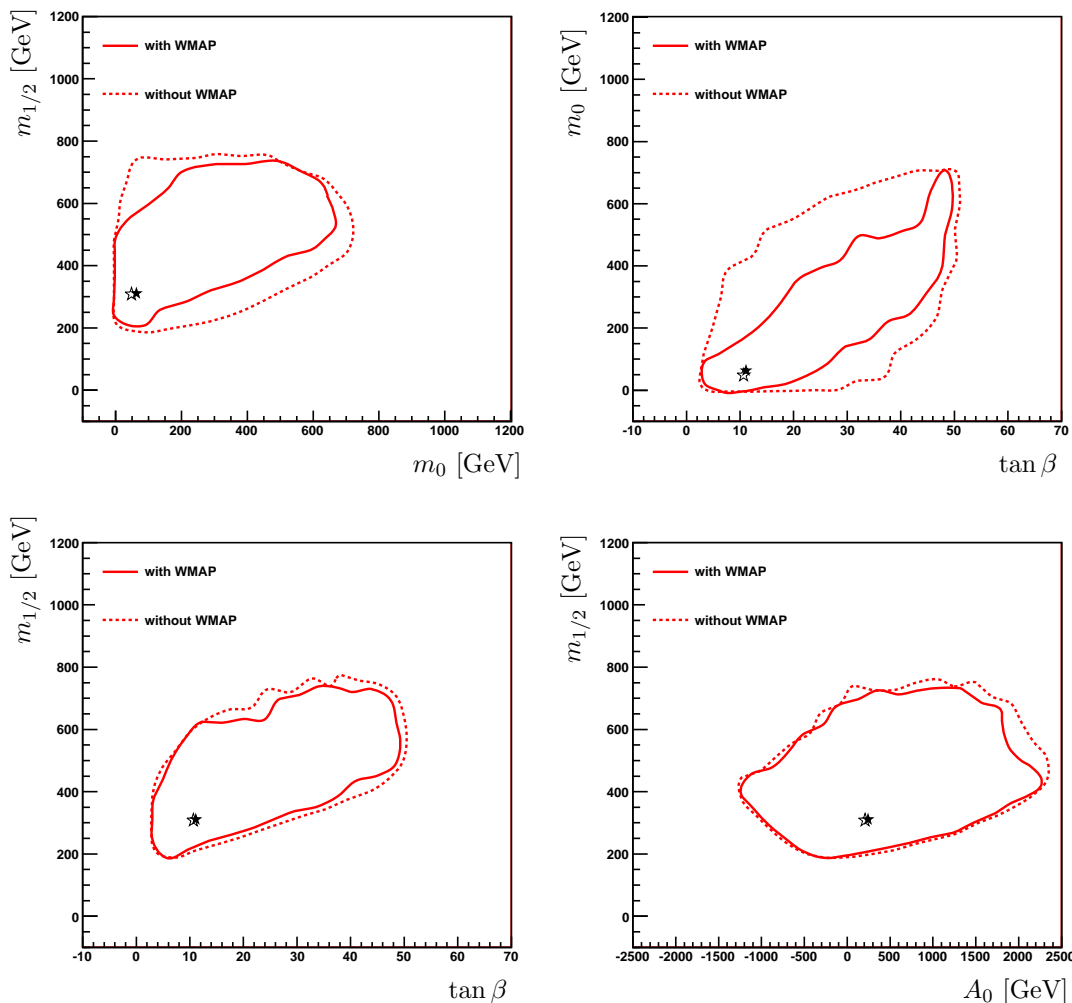
Figure 3: Variation of the 95% C.L. allowed regions in the MSSM parameter space including (solid) or excluding (dotted) the WMAP constraint. The plots show the $(m_0, m_{1/2})$ plane (upper left), $(\tan\beta, m_0)$ plane (upper right), $(\tan\beta, m_{1/2})$ plane (lower left) and the $(A_0, m_{1/2})$ plane (lower right plot). In each panel, we mark the best-fit points found both with and without the WMAP constraint by a filled and open star, respectively.

example, the value of m_0 favoured by $\Omega_{\rm CDM}$ for any given values of $m_{1/2}$ and A_0 increases as the value of $\tan\beta$ increases, foliating the $(m_0, m_{1/2})$ plane. Thus, for any given value of $m_{1/2}$ and A_0, a large range of values of m_0 can be attained for a suitable choice of $\tan\beta$, even if one does impose the $\Omega_{\rm CDM}$ constraint. Concerning the range of $m_{1/2}$, this is bounded above by $(g-2)_\mu$, and, for any given value of $\tan\beta$, the allowed range actually decreases for the larger values of m_0 allowed if the $\Omega_{\rm CDM}$ constraint is dropped. Thus, dropping the $\Omega_{\rm CDM}$ constraint has little overall effect on the ranges of $m_{1/2}$, m_0 and A_0. The primary effect is to enforce a correlation between $\tan\beta$ and m_0, as seen in the upper right panel of figure 3. The range of m_0 decreases at any fixed value of $\tan\beta$ when the $\Omega_{\rm CDM}$ constraint is imposed, because of the narrowness of the WMAP strip for any fixed value of $\tan\beta$.

Thus, we find that the fit results obtained in the parameter planes of m_0, $m_{1/2}$, A_0
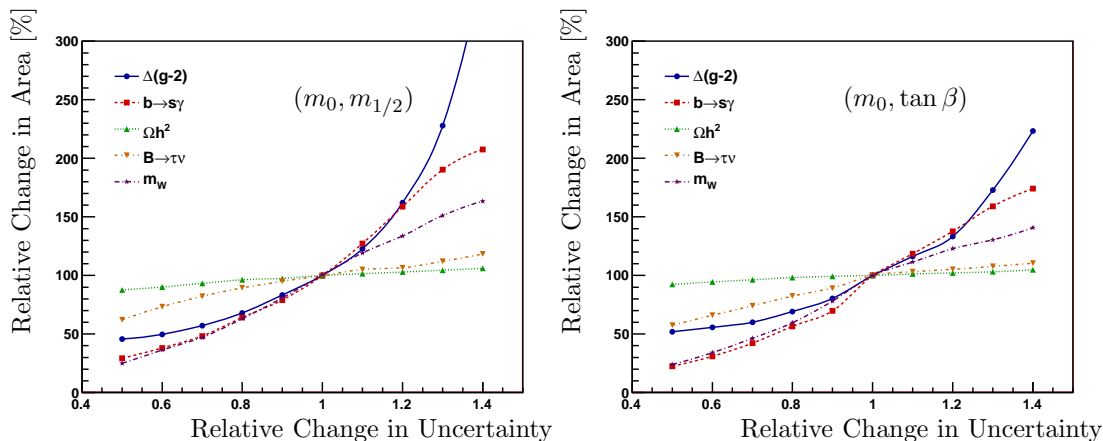
Figure 4: Relative sizes of the 95% C.L. areas in the $(m_0, m_{1/2})$ plane (left) and in the $(m_0, \tan\beta)$ plane (right) as a function of the hypothetical errors of $(g-2)_\mu$, $\mathrm{BR}(b \to s\gamma)$, $\Omega_{\mathrm{CDM}}h^2$, $\mathrm{BR}(B_u \to \tau\nu_\tau)$, m_W. The error scaling is relative to the current combined theory and experimental error.

and $\tan\beta$ displayed in figure 1 are rather robust with respect to imposing / dropping the Ω_{CDM} constraint. On the other hand, as already noted, the Ω_{CDM} constraint does reduce the dimensionality of the parameter space by essentially one unit. This can also be seen from the fact that without imposing the Ω_{CDM} constraint the preferred parameter region obtained from the fit to the EWPO and BPO still yields a wide range of possible values of $\Omega_{\mathrm{CDM}}h^2$. Specifically we find that the 68% C.L. region of the $(m_0, m_{1/2})$ plane shown in figure 1 yields $\Omega_{\mathrm{CDM}}h^2 < 0.9$, while considerably larger values of $\Omega_{\mathrm{CDM}}h^2$ are allowed at the 95% C.L. Eventually, SUSY particle mass measurements at the LHC (see the discussion of figure 6 below) may enable this estimate of $\Omega_{\mathrm{CDM}}h^2$ to be refined considerably (see, e.g., [106, 111, 112]).

Drilling down into the dependences of our results on uncertainties in the experimental and phenomenological constraints, we display in figure 4 the results of studies of their sensitivities to some key observables. The observables tracked are $(g-2)_\mu$, $\mathrm{BR}(b \to s\gamma)$, $\Omega_{\mathrm{CDM}}h^2$, $\mathrm{BR}(B_u \to \tau\nu_\tau)$ and m_W. The left panel shows the percentage variation in the preferred region of the $(m_0, m_{1/2})$ plane as the assumed errors in these quantities are rescaled, assuming that the future experimental central values agree with the current ones. The right panel shows the same for the area in the $(m_0, \tan\beta)$ plane. Larger errors could arise if we have underestimated the relevant systematic errors, and smaller errors could result from future improvements of the experimental errors and/or the theoretical predictions. As could be expected from the discussion in the previous paragraph, the preferred areas vary very little with the error in Ω_{CDM}, and the areas are also relatively insensitive to that in $\mathrm{BR}(B_u \to \tau\nu_\tau)$. However, there are greater sensitivities to $\mathrm{BR}(b \to s\gamma)$, m_W and (particularly) $(g-2)_\mu$.

The theoretical error in m_W is much smaller than the current experimental error. It is encouraging that reducing the experimental error, as should be possible with future Tevatron and LHC data, could have substantial effects on the preferred areas in the parameter planes. A reduction in the error by a factor two could reduce the areas by factors of about five, if the present central value (which disagrees with the SM by about one σ) is maintained.

The same would be true for a reduction in the error in $BR(b \to s\gamma)$, but here reducing the theoretical error would also be necessary. This would require, in particular, a better understanding of the uncertainties in higher-order and non-perturbative QCD corrections. Indeed, a very conservative approach to the combination of the current theoretical and experimental errors in $BR(b \to s\gamma)$ might even motivate a larger error and hence larger preferred areas than in our default analysis.

Figure 4 also shows that varying the error in $(g-2)_\mu$ is potentially more important, particularly if the present error is underestimated. This might be the case if, e.g., the weight of experimental evidence would shift towards using τ decay data to estimate the SM hadronic contribution to $(g-2)_\mu$, or if the error in the light-by-light contribution were to be revised drastically.[6] The rapid increases in the areas of the preferred regions reflect the fact that a more relaxed treatment of the $(g-2)_\mu$ error led in the past to (parts) of the focus-point strip at large m_0 being included within the preferred region, which does not occur in our default analysis.

In order to explore the sensitivity to the $(g-2)_\mu$ error in more detail, we show in the left panel of figure 5 the effect in the CMSSM $(m_0, m_{1/2})$ plane of varying this error, while assuming the same central value. Going from the outer to the inner contours we have assumed $\sigma_{\text{hypothetical}}/\sigma_{\text{today}} = 1.3, 1.2, 1.1, 1.0, 0.9, 0.7$ with $\sigma_{\text{today}} = 8.8 \times 10^{-10}$, see table 1. The partially fuzzy shapes would be smoothed by higher statistics. We see that the preferred region expands rapidly if the $(g-2)_\mu$ error is increased. Going to an increase by a factor of 1.5 (not shown in the plot) would open up the focus-point region, which is disfavoured in our analysis. Conversely, decreasing this error, as would be possible with an accessible improvement of the previous BNL $(g-2)_\mu$ experiment [56], would enable the preferred ranges of the CMSSM mass parameters to be decreased impressively. Ultimately, this together with the other EWPO and BPO could make possible a sensitive test of SUSY at the loop level, if the LHC does indeed discover sparticles and measure their masses.

In the right panel of figure 5, we make a similar analysis of the sensitivity to the $BR(b \to s\gamma)$ error. Going from the outer to the inner contours we have again assumed $\sigma_{\text{hypothetical}}/\sigma_{\text{today}} = 1.3, 1.2, 1.1, 1.0, 0.9, 0.7$ with $\sigma_{\text{today}}(BR_{b \to s\gamma}^{\text{exp}}/BR_{b \to s\gamma}^{\text{SM}}) = 0.12$, see table 1. We see from the right panel of figure 5 that treating the errors differently could have a significant effect. Employing a larger error (as done in [39], for instance), would not only expand the allowed regions, but also allow larger $\tan\beta$ values, as $BR(b \to s\gamma)$ is particularly sensitive to $\tan\beta$.

Though in the present analysis we have focused on the $\mu > 0$ solution, as favoured by the $(g-2)_\mu$ anomaly, we comment briefly here on the structure of the $\mu < 0$ parameter space. In order to minimize the discrepancy with the $(g-2)_\mu$ constraint, for $\mu < 0$ one would need a relatively heavy spectrum in order to suppress the SUSY effects with the wrong sign. This would be particularly true for increasing values of $\tan\beta$, since $(g-2)_\mu$ grows almost linearly with $\tan\beta$. $BR(b \to s\gamma)$ is also highly sensitive to the sign of the μ parameter. In particular, within the CMSSM the solution with $\mu < 0$ unambiguously implies that all

---

[6]In [13] it has recently been claimed that solving the muon $(g-2)_\mu$ anomaly by changing the SM prediction of the hadronic contribution to $(g-2)_\mu$ is unlikely in view of a combined analysis of all electroweak data.
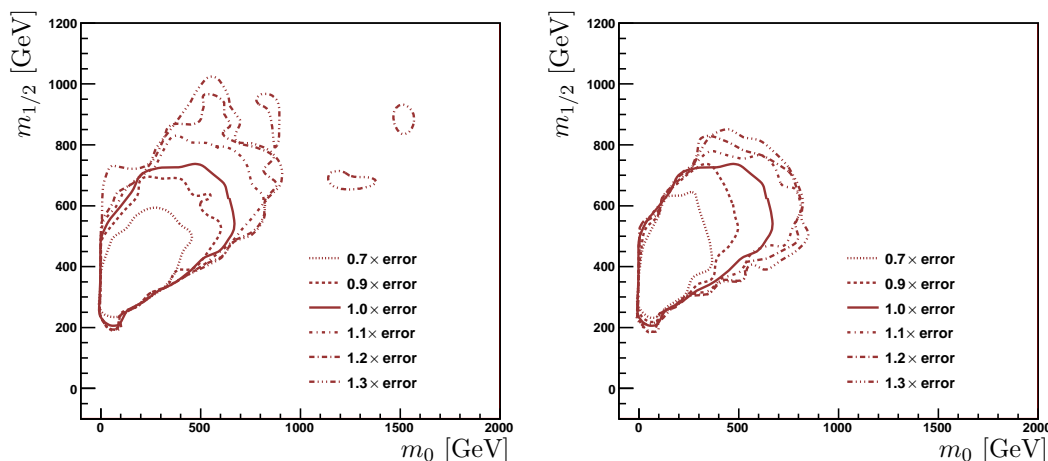
Figure 5: The 95% C.L. region in the $(m_0, m_{1/2})$ plane for various hypothetical values of the 1σ uncertainty (combined theory and experimental) of $(g-2)_\mu$(left) and BR($b \to s\gamma$)(right). The curves show (from outer to inner) the 95% C.L. regions for $\sigma_{\text{hypothetical}}/\sigma_{\text{today}} = 1.3, 1.2, 1.1, 1.0, 0.9, 0.7$ for $\sigma_{\text{today}} = 8.8 \times 10^{-10}$ (left) and $\sigma_{\text{today}}(\text{BR}^{\text{exp}}_{\text{b}\to\text{s}\gamma}/\text{BR}^{\text{SM}}_{\text{b}\to\text{s}\gamma}) = 0.12$ (right), respectively, see table 1.

the dominant SUSY effects to BR($b \to s\gamma$) have the same sign and interfere constructively with the SM amplitude. This implies more severe constrains with respect to the $\mu > 0$ case, and again points toward a heavy spectrum. This is not the case for $\mu > 0$, where partial cancellations among SUSY effects in BR($b \to s\gamma$) allow relatively light squarks.

We have also considered possible improvements in the determination of the CMSSM parameters that might be obtainable from early LHC measurements. Missing E_T measurements with or without single leptons are unlikely to constrain the model with high precision. On the other hand, in the parameter region preferred by the fit (with $\tan\beta \approx 10$) there are good prospects for measuring the opposite-sign dilepton edge in $\tilde{\chi}_2 \to \tilde{\chi}_1 \ell^+\ell^-$ ($\ell = e, \mu$) decays with high precision, which is located at

$$(m_{\ell\ell}^2)^{\text{edge}} = \frac{(m_{\tilde{\chi}_2^0}^2 - m_{\tilde{\ell}_R}^2)(m_{\tilde{\ell}_R}^2 - m_{\tilde{\chi}_1^0}^2)}{m_{\tilde{\ell}_R}^2}. \tag{3.1}$$

Such a measurement would constrain a combination of sparticle masses and hence the CMSSM parameter space in an interesting way. As an appetizer for what might be possible, we show in figure 6 the possible impact of a measurement of the dilepton edge for the CMSSM best-fit point described in the previous paragraph, which has $m_{\tilde{\chi}_1^0} = 121$ GeV, $m_{\tilde{\chi}_2^0} = 225$ GeV, $m_{\tilde{l}_R} = 139$ GeV, yielding an edge at $m_{\ell^+\ell^-} = 87$ GeV. We assume experimental and theoretical errors of 3 GeV each. We see in figure 6 that the dilepton edge measurement would reduce the parameter space preferred at the 68% C.L. to two narrow strips in the $(m_0, m_{1/2})$ plane, linked into a tilted 'vee' shape at the 95% C.L. The best-fit point in the right wing of the 'vee' has quite different parameter values from the overall best-fit point in the left wing of the 'vee': $m_{1/2} = 390$ GeV, $m_0 = 230$ GeV, $A_0 = 1230$ GeV, $\tan\beta = 23$, yielding $\chi^2 = 22.7$ and $m_{\tilde{\chi}_1^0} = 155$ GeV, $m_{\tilde{\chi}_2^0} = 293$ GeV, $m_{\tilde{l}_R} = 273$ GeV.
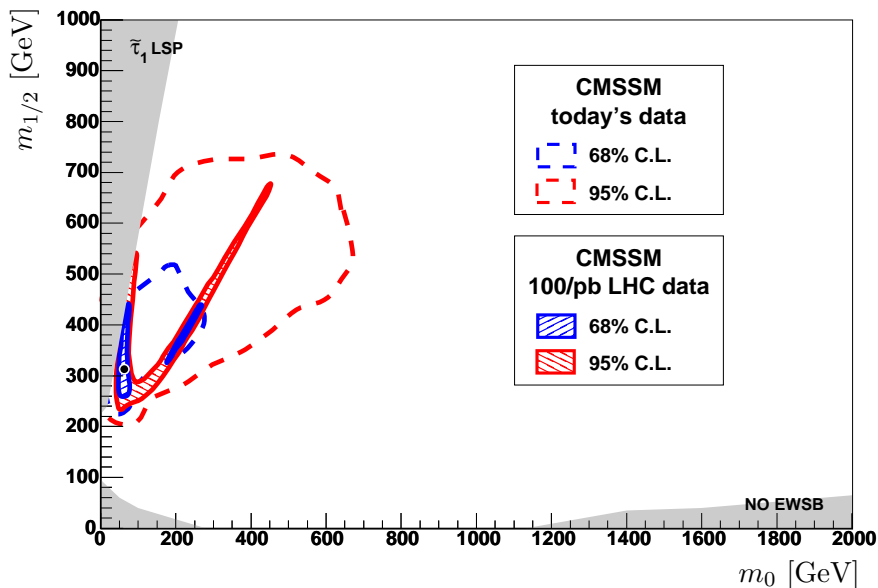
Figure 6: The $(m_0, m_{1/2})$ plane in the CMSSM for $\tan\beta = 10$ and $A_0 = 0$, showing the improvement in the constraints on m_0 and $m_{1/2}$ that could be obtained by measuring the opposite-sign dilepton edge with $1\,\mathrm{fb}^{-1}$ of integrated luminosity at $14\,\mathrm{TeV}$, assuming the spectrum of the best-fit point shown in the left panel of figure 2, and experimental and theoretical errors of $3\,\mathrm{GeV}$ each. The best-fit point is indicated by a filled circle.

3.3 Comparison with the NUHM1 case

The above analysis of the CMSSM is relatively encouraging for the early days of the LHC, but one might wonder to what extent the conclusions can be extended to more general incarnations of the MSSM. The full parameter space of the MSSM has so many dimensions that exploring it with the MCMC approach used here would require prohibitive amounts of CPU time. Accordingly, we discuss briefly here only the simplest possible generalization of the CMSSM, in which the soft supersymmetry-breaking scalar contributions to the Higgs masses are allowed to differ by the same amount from those of the squarks and sleptons at the GUT scale, the so-called non-universal Higgs model 1 (NUHM1) [113–115].

Overall, it is encouraging that the general sizes of the 68% and 95% C.L. regions are similar to those in the CMSSM, as shown in figure 7, though the 68% C.L. region together with the best-fit point are shifted to lower $m_{1/2}$, and the 95% C.L. region is more elongated in $m_{1/2}$. As in the case of the CMSSM, SUSY could be discovered over all of the 68% C.L. region with 100 pb^{-1} of integrated luminosity at $14\,\mathrm{TeV}$ in a single experiment, and even 50 pb^{-1} of integrated luminosity at $10\,\mathrm{TeV}$ would cover most of it. As in the CMSSM, not all of the NUHM1 95% C.L. region would be covered by the LHC with $1\,\mathrm{fb}^{-1}$ of integrated luminosity at $14\,\mathrm{TeV}$, whereas the same-sign dilepton search would cover all the 68% C.L. region in the NUHM1. There are differences between the shapes of the preferred regions in the CMSSM and the NUHM1, particularly at low $m_{1/2}$. This reflects the fact that the Ω_{CDM} constraint can be obeyed away from the coannihilation strip at larger values of m_0, if $m_\chi \sim m_{H/A}/2$. This freedom can then be exploited to relax the slight tension induced by m_h which arises in the CMSSM.

The spectrum at the best-fit NUHM1 point is shown in the right panel of figure 2.
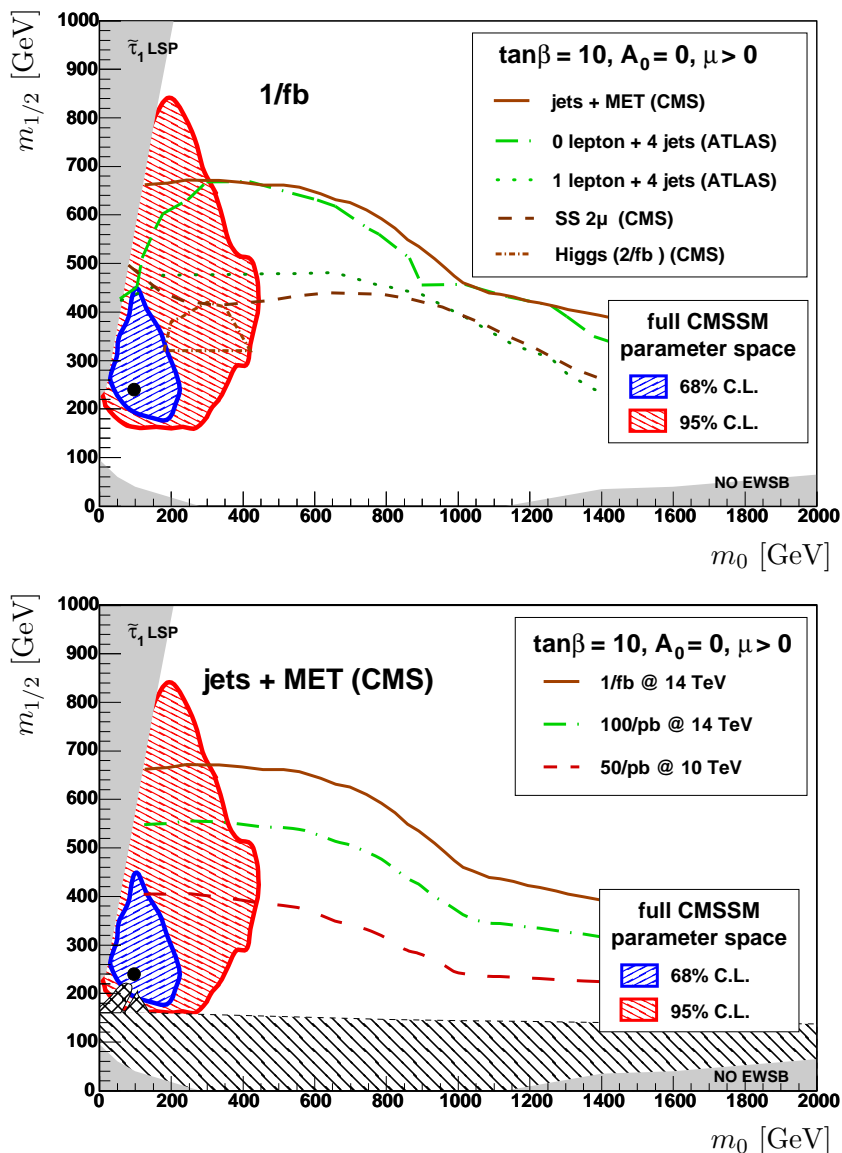
Figure 7: The $(m_0, m_{1/2})$ plane in the CMSSM for $\tan\beta = 10$ and $A_0 = 0$, as in figure 1, overlaid with the 68% and 95% probability contours for the NUHM1. Upper plot: Some $5\,\sigma$ discovery contours at ATLAS and CMS with $1\,\text{fb}^{-1}$ at $14\,\text{TeV}$, and the contour for the $5\,\sigma$ discovery of the Higgs boson in sparticle decays with $2\,\text{fb}^{-1}$ at $14\,\text{TeV}$ in CMS. Lower plot: The $5\,\sigma$ discovery contours for jet + missing E_T events at CMS with $1\,\text{fb}^{-1}$ at $14\,\text{TeV}$, $100\,\text{pb}^{-1}$ at $14\,\text{TeV}$ and $50\,\text{pb}^{-1}$ at $10\,\text{TeV}$ centre-of-mass energy.

This point has $m_0 = 100\,\text{GeV}$, $m_{1/2} = 240\,\text{GeV}$, $A_0 = -930\,\text{GeV}$, $\tan\beta = 7$, $m_H^2 = -6.9 \times 10^5\,\text{GeV}^2$ and $\mu = 870\,\text{GeV}$, yielding $\chi^2 = 18.0$ (39% probability) and $m_h = 118\,\text{GeV}$. The best-fit values of $m_{1/2}$ and $\tan\beta$ are somewhat lower than those in the CMSSM, whereas the value of m_0 is somewhat higher. The overall value of χ^2 is also somewhat lower than in the CMSSM, reflecting the relaxation of the slight tension in the value of m_h that is possible when the Higgs masses are allowed to become non-universal. Comparing with the best-fit CMSSM spectrum, we see that the masses of the sleptons and squarks are quite similar, as are the masses of the lighter neutralinos and chargino. However, the

splitting between the stop mass eigenstates is larger — reflecting the larger value of $|A_0|$, the heavier neutralinos and chargino are much heavier — reflecting the larger value of μ, the best-fit value of m_h lies comfortably above the LEP lower limit, and the heavier Higgs bosons are lighter than in the CMSSM — reflecting the extra freedom conferred by the non-universality in the NUHM1. The lower values of the heavier Higgs masses compensate other SUSY contributions to BR($b \to s\gamma$), and offer better prospects for detection at the LHC than those offered by the CMSSM.

4. Conclusion and outlook

Making a probabilistic analysis using a MCMC technique, we have presented in this paper the regions preferred in the CMSSM and the NUHM1 parameter spaces at the 68% and 95% C.L., as well as the spectra at the best-fit points, in the light of the present direct and indirect constraints on the models' parameters. Particularly important roles are played by $(g-2)_\mu$ and BR($b \to s\gamma$), and we have analyzed the ways in which effects of these constraints vary with the sizes of their theoretical uncertainties and experimental errors. We have quantified how strengthening (or relaxing) either of these constraints would reduce (or expand) considerably the preferred regions in the CMSSM $(m_0, m_{1/2})$ plane. We have also studied the impact of the constraint on the cold dark matter density imposed by WMAP. We find that the results for the best-fit points are remarkably robust with respect to imposing or dropping the constraint on the cold dark matter density. Perhaps surprisingly, we find that this constraint does not restrict significantly most two-dimensional projections of the preferred region in the CMSSM parameter space. Encouragingly, we find that the preferred regions in the NUHM1 are quite similar to those in the CMSSM.

The 95% exclusion regions in the $(m_0, m_{1/2})$ plane extend significantly further than the discovery regions shown above. Therefore, if SUSY were to be excluded at the LHC with $1\,\text{fb}^{-1}$ ($100\,\text{pb}^{-1}$) of integrated luminosity at $14\,\text{TeV}$, the 95% (68%) C.L. regions in both the CMSSM and the NUHM1 would be ruled out. On the other hand, SUSY could be discovered at the $5\,\sigma$ level at the LHC with $1\,\text{fb}^{-1}$ of integrated luminosity at $14\,\text{TeV}$ in a single experiment over most of the 95% C.L. regions in the $(m_0, m_{1/2})$ planes of the CMSSM and the NUHM1. Only the highest $m_{1/2}$ values would require a larger integrated luminosity, or the combination of data from both ATLAS and CMS. Indeed, SUSY could be discovered over all of the 68% C.L. regions in both the CMSSM and the NUHM1 with just $100\,\text{pb}^{-1}$ of integrated luminosity at $14\,\text{TeV}$, and even $50\,\text{pb}^{-1}$ of (good-quality) data at $10\,\text{TeV}$ would offer significant prospects for SUSY detection. The same-sign dilepton search would cover most (all) of the 68% C.L. region in the CMSSM (NUHM1). If Nature were to choose the best-fit CMSSM point, a measurement of the same-sign dilepton endpoint would impose a strong constraint on the SUSY spectrum.

One way or the other, there are good prospects that the initial runs of the LHC will determine the fate of many speculations about the relevance of low-energy SUSY to particle physics.

Acknowledgments

References

[1] H.P. Nilles, *Supersymmetry, supergravity and particle physics*, *Phys. Rept.* **110** (1984) 1.

[2] H.E. Haber and G.L. Kane, *The search for supersymmetry: probing physics beyond the standard model*, *Phys. Rept.* **117** (1985) 75.

[3] R. Barbieri, S. Ferrara and C.A. Savoy, *Gauge models with spontaneously broken local supersymmetry*, *Phys. Lett.* **B 119** (1982) 343.

[4] PARTICLE DATA GROUP collaboration, C. Amsler et al., *Review of particle physics*, *Phys. Lett.* **B 667** (2008) 1.

[5] LEP WORKING GROUP FOR HIGGS BOSON SEARCHES collaboration, R. Barate et al., *Search for the standard model Higgs boson at LEP*, *Phys. Lett.* **B 565** (2003) 61 [hep-ex/0306033].

[6] ALEPH collaboration, S. Schael et al., *Search for neutral MSSM Higgs bosons at LEP*, *Eur. Phys. J.* **C 47** (2006) 547 [hep-ex/0602042].

[7] MUON G-2 collaboration, G.W. Bennett et al., *Final report of the muon E821 anomalous magnetic moment measurement at BNL*, *Phys. Rev.* **D 73** (2006) 072003 [hep-ex/0602035].

[8] T. Moroi, *The muon anomalous magnetic dipole moment in the minimal supersymmetric standard model*, *Phys. Rev.* **D 53** (1996) 6565 [*Erratum ibid.* **56** (1997) 4424] [hep-ph/9512396].

[9] A. Czarnecki and W.J. Marciano, *The muon anomalous magnetic moment: a harbinger for 'new physics'*, *Phys. Rev.* **D 64** (2001) 013014 [hep-ph/0102122].

[10] M. Davier, *The hadronic contribution to* $(g-2)_\mu$, *Nucl. Phys.* **169** *(Proc. Suppl.)* (2007) 288 [hep-ph/0701163].

[11] J.P. Miller, E. de Rafael and B.L. Roberts, *Muon* $g-2$: *review of theory and experiment*, *Rept. Prog. Phys.* **70** (2007) 795 [hep-ph/0703049].

[12] F. Jegerlehner, *Essentials of the muon* $g-2$, *Acta Phys. Polon.* **B38** (2007) 3021 [hep-ph/0703125].

[13] M. Passera, W.J. Marciano and A. Sirlin, *The muon* $g-2$ *and the bounds on the Higgs boson mass*, *Phys. Rev.* **D 78** (2008) 013009 [arXiv:0804.1142].

[14] WMAP collaboration, J. Dunkley et al., *Five-year Wilkinson Microwave Anisotropy Probe (WMAP) observations: likelihoods and parameters from the WMAP data*, arXiv:0803.0586.

[15] B.C. Allanach and C.G. Lester, *Sampling using a 'bank' of clues*, *Comput. Phys. Commun.* **179** (2008) 256 [arXiv:0705.0486].

[16] A. Djouadi, M. Drees and J.L. Kneur, *Constraints on the minimal supergravity model and prospects for SUSY particle production at future linear e^+e^- colliders*, *JHEP* **08** (2001) 055 [hep-ph/0107316].

[17] W. de Boer, M. Huber, C. Sander and D.I. Kazakov, *A global fit to the anomalous magnetic moment, $b \to X_s\gamma$ and Higgs limits in the constrained MSSM*, *Phys. Lett.* **B 515** (2001) 283.

[18] W. de Boer and C. Sander, *Global electroweak fits and gauge coupling unification*, *Phys. Lett.* **B 585** (2004) 276 [hep-ph/0307049].

[19] J.R. Ellis, K.A. Olive and Y. Santoso, *Constraining supersymmetry*, *New J. Phys.* **4** (2002) 32 [hep-ph/0202110].

[20] H. Baer et al., *Updated constraints on the minimal supergravity model*, *JHEP* **07** (2002) 050 [hep-ph/0205325].

[21] R.L. Arnowitt and B. Dutta, *Dark matter, muon $g-2$ and other accelerator constraints*, hep-ph/0211417.

[22] J.R. Ellis, K.A. Olive, Y. Santoso and V.C. Spanos, *Supersymmetric dark matter in light of WMAP*, *Phys. Lett.* **B 565** (2003) 176 [hep-ph/0303043].

[23] H. Baer and C. Balázs, *χ^2 analysis of the minimal supergravity model including WMAP, $g_\mu - 2$ and $b \to s\gamma$ constraints*, *JCAP* **05** (2003) 006 [hep-ph/0303114].

[24] A.B. Lahanas and D.V. Nanopoulos, *WMAPing out supersymmetric dark matter and phenomenology*, *Phys. Lett.* **B 568** (2003) 55 [hep-ph/0303130].

[25] U. Chattopadhyay, A. Corsetti and P. Nath, *WMAP constraints, SUSY dark matter and implications for the direct detection of SUSY*, *Phys. Rev.* **D 68** (2003) 035005 [hep-ph/0303201].

[26] C. Muñoz, *Dark matter detection in the light of recent experimental results*, *Int. J. Mod. Phys.* **A 19** (2004) 3093 [hep-ph/0309346].

[27] G. Bélanger, F. Boudjema, A. Cottrant, A. Pukhov and A. Semenov, *WMAP constraints on SUGRA models with non-universal gaugino masses and prospects for direct detection*, *Nucl. Phys.* **B 706** (2005) 411 [hep-ph/0407218].

[28] J.R. Ellis, K.A. Olive, Y. Santoso and V.C. Spanos, *Likelihood analysis of the CMSSM parameter space*, *Phys. Rev.* **D 69** (2004) 095004 [hep-ph/0310356].

[29] J.R. Ellis, S. Heinemeyer, K.A. Olive and G. Weiglein, *Indirect sensitivities to the scale of supersymmetry*, *JHEP* **02** (2005) 013 [hep-ph/0411216].

[30] J.R. Ellis, D.V. Nanopoulos, K.A. Olive and Y. Santoso, *On the Higgs mass in the CMSSM*, *Phys. Lett.* **B 633** (2006) 583 [hep-ph/0509331].

[31] J.R. Ellis, S. Heinemeyer, K.A. Olive and G. Weiglein, *Phenomenological indications of the scale of supersymmetry*, *JHEP* **05** (2006) 005 [hep-ph/0602220].

[32] J.R. Ellis, S. Heinemeyer, K.A. Olive, A.M. Weber and G. Weiglein, *The supersymmetric parameter space in light of b-physics observables and electroweak precision data*, *JHEP* **08** (2007) 083 [arXiv:0706.0652].

[33] J.R. Ellis, S. Heinemeyer, K.A. Olive and G. Weiglein, *Light heavy MSSM Higgs bosons at large* $\tan\beta$, *Phys. Lett.* **B 653** (2007) 292 [arXiv:0706.0977].

[34] E.A. Baltz and P. Gondolo, *Markov chain Monte Carlo exploration of minimal supergravity with implications for dark matter*, *JHEP* **10** (2004) 052 [hep-ph/0407039].

[35] B.C. Allanach and C.G. Lester, *Multi-dimensional mSUGRA likelihood maps*, *Phys. Rev.* **D 73** (2006) 015013 [hep-ph/0507283].

[36] B.C. Allanach, *Naturalness priors and fits to the constrained minimal supersymmetric standard model*, *Phys. Lett.* **B 635** (2006) 123 [hep-ph/0601089].

[37] B.C. Allanach, C.G. Lester and A.M. Weber, *The dark side of mSUGRA*, *JHEP* **12** (2006) 065 [hep-ph/0609295].

[38] B.C. Allanach, K. Cranmer, C.G. Lester and A.M. Weber, *Natural priors, CMSSM fits and LHC weather forecasts*, *JHEP* **08** (2007) 023 [arXiv:0705.0487].

[39] F. Feroz et al., *Bayesian selection of* sign(μ) *within mSUGRA in global fits including WMAP5 results*, arXiv:0807.4512.

[40] R.R. de Austri, R. Trotta and L. Roszkowski, *A Markov chain Monte Carlo analysis of the CMSSM*, *JHEP* **05** (2006) 002 [hep-ph/0602028].

[41] L. Roszkowski, R.R. de Austri and R. Trotta, *On the detectability of the CMSSM light Higgs boson at the Tevatron*, *JHEP* **04** (2007) 084 [hep-ph/0611173].

[42] L. Roszkowski, R. Ruiz de Austri and R. Trotta, *Implications for the constrained MSSM from a new prediction for* $b \to s\gamma$, *JHEP* **07** (2007) 075 [arXiv:0705.2012].

[43] L. Roszkowski, R.R. de Austri, J. Silk and R. Trotta, *On prospects for dark matter indirect detection in the constrained MSSM*, arXiv:0707.0622.

[44] S. Heinemeyer, X. Miao, S. Su and G. Weiglein, *B-physics observables and electroweak precision data in the CMSSM, mGMSB and mAMSB*, arXiv:0805.2359.

[45] P. Bechtle, K. Desch and P. Wienemann, *Fittino, a program for determining MSSM parameters from collider observables using an iterative method*, *Comput. Phys. Commun.* **174** (2006) 47 [hep-ph/0412012].

[46] R. Lafaye, T. Plehn, M. Rauch and D. Zerwas, *Measuring supersymmetry*, *Eur. Phys. J.* **C 54** (2008) 617 [arXiv:0709.3985].

[47] O. Buchmueller et al., *Prediction for the lightest Higgs boson mass in the CMSSM using indirect experimental constraints*, *Phys. Lett.* **B 657** (2007) 87 [arXiv:0707.3447].

[48] B.C. Allanach and D. Hooper, *Panglossian prospects for detecting neutralino dark matter in light of natural priors*, arXiv:0806.1923.

[49] R. Trotta, *SuperBayeS. Bayesian inference for supersymmetric parameter constraints*, talk given at *Tools08, tools for the new physics and its background*, Munich Germany June 30 – July 4 2008, http://indico.cern.ch/getFile.py/access?contribId=43&sessionId=20&resId=0 &materialId=slides&confId=35476, based on work done in collaboration with L. Roszkowski and R.R. de Austri.

[50] S. Heinemeyer, W. Hollik, D. Stöckinger, A.M. Weber and G. Weiglein, *Precise prediction for M(W) in the MSSM*, *JHEP* **08** (2006) 052 [hep-ph/0604147].

[51] S. Heinemeyer, W. Hollik, A.M. Weber and G. Weiglein, *Z pole observables in the MSSM*, *JHEP* **04** (2008) 039 [`arXiv:0710.2972`].

[52] M. Verzocchi, *Electroweak physics (includes W mass & width, WW, WZ, ZZ)*, talk at *ICHEP* 2008, Philadelphia U.S.A. July 29 – August 5 2008.

[53] G. Degrassi and G.F. Giudice, *QED logarithms in the electroweak corrections to the muon anomalous magnetic moment*, *Phys. Rev.* **D 58** (1998) 053007 [`hep-ph/9803384`].

[54] S. Heinemeyer, D. Stöckinger and G. Weiglein, *Two-loop SUSY corrections to the anomalous magnetic moment of the muon*, *Nucl. Phys.* **B 690** (2004) 62 [`hep-ph/0312264`].

[55] S. Heinemeyer, D. Stöckinger and G. Weiglein, *Electroweak and supersymmetric two-loop corrections to* $(g-2)_\mu$, *Nucl. Phys.* **B 699** (2004) 103 [`hep-ph/0405255`].

[56] D.W. Hertzog, J.P. Miller, E. de Rafael, B. Lee Roberts and D. Stöckinger, *The physics case for the new muon* $(g-2)$ *experiment*, `arXiv:0705.4617`.

[57] G. Degrassi, S. Heinemeyer, W. Hollik, P. Slavich and G. Weiglein, *Towards high-precision predictions for the MSSM Higgs sector*, *Eur. Phys. J.* **C 28** (2003) 133 [`hep-ph/0212020`].

[58] S. Heinemeyer, W. Hollik and G. Weiglein, *The masses of the neutral CP-even Higgs bosons in the MSSM: accurate analysis at the two-loop level*, *Eur. Phys. J.* **C 9** (1999) 343 [`hep-ph/9812472`].

[59] S. Heinemeyer, W. Hollik and G. Weiglein, *FeynHiggs: a program for the calculation of the masses of the neutral CP-even Higgs bosons in the MSSM*, *Comput. Phys. Commun.* **124** (2000) 76 [`hep-ph/9812320`];
see http://www.feynhiggs.de.

[60] M. Frank et al., *The Higgs boson masses and mixings of the complex MSSM in the Feynman-diagrammatic approach*, *JHEP* **02** (2007) 047 [`hep-ph/0611326`].

[61] M. Misiak et al., *The first estimate of* $B(\bar{B} \to X_s\gamma)$ *at* $O(\alpha_s^2)$, *Phys. Rev. Lett.* **98** (2007) 022002 [`hep-ph/0609232`].

[62] M. Ciuchini, G. Degrassi, P. Gambino and G.F. Giudice, *Next-to-leading QCD corrections to* $B \to X_s\gamma$ *in supersymmetry*, *Nucl. Phys.* **B 534** (1998) 3 [`hep-ph/9806308`].

[63] G. Degrassi, P. Gambino and G.F. Giudice, $B \to X_s\gamma$ *in supersymmetry: large contributions beyond the leading order*, *JHEP* **12** (2000) 009 [`hep-ph/0009337`].

[64] M.S. Carena, D. Garcia, U. Nierste and C.E.M. Wagner, $b \to s\gamma$ *and supersymmetry with large* $\tan\beta$, *Phys. Lett.* **B 499** (2001) 141 [`hep-ph/0010003`].

[65] G. D'Ambrosio, G.F. Giudice, G. Isidori and A. Strumia, *Minimal flavour violation: an effective field theory approach*, *Nucl. Phys.* **B 645** (2002) 155 [`hep-ph/0207036`].

[66] HEAVY FLAVOR AVERAGING GROUP (HFAG) collaboration, E. Barberio et al., *Averages of b-hadron properties at the end of* 2005, `hep-ex/0603003`.

[67] TEVATRON ELECTROWEAK WORKING GROUP collaboration and others, *Combination of CDF and D0 results on the mass of the top quark*, `arXiv:0808.1089`.

[68] G. Bélanger, F. Boudjema, A. Pukhov and A. Semenov, *MicrOMEGAs2.0: a program to calculate the relic density of dark matter in a generic model*, *Comput. Phys. Commun.* **176** (2007) 367 [`hep-ph/0607059`].

[69] G. Bélanger, F. Boudjema, A. Pukhov and A. Semenov, *MicrOMEGAs: a program for calculating the relic density in the MSSM, Comput. Phys. Commun.* **149** (2002) 103 [`hep-ph/0112278`].

[70] G. Bélanger, F. Boudjema, A. Pukhov and A. Semenov, *MicrOMEGAs: version* 1.3, *Comput. Phys. Commun.* **174** (2006) 577 [`hep-ph/0405253`].

[71] G. Isidori and A. Retico, *Scalar flavour-changing neutral currents in the large-*$\tan\beta$ *limit, JHEP* **11** (2001) 001 [`hep-ph/0110121`].

[72] A.J. Buras, P.H. Chankowski, J. Rosiek and L. Slawianowska, $\Delta(M_{(d,s)})$, $B^0_{(d,s)} \to \mu^+\mu^-$ *and* $B \to X_s\gamma$ *in supersymmetry at large* $\tan\beta$, *Nucl. Phys.* **B 659** (2003) 3 [`hep-ph/0210145`].

[73] G. Isidori and P. Paradisi, *Hints of large* $\tan\beta$ *in flavour physics, Phys. Lett.* **B 639** (2006) 499 [`hep-ph/0605012`].

[74] G. Isidori, F. Mescia, P. Paradisi and D. Temes, *Flavour physics at large* $\tan\beta$ *with a Bino-like LSP, Phys. Rev.* **D 75** (2007) 115019 [`hep-ph/0703035`] and references therein.

[75] A.G. Akeroyd and S. Recksiegel, *The effect of* $H^\pm$ *on* $B^\pm \to \tau^\pm\nu_\tau$ *and* $B^\pm \to \mu^\pm\nu_\mu$, *J. Phys.* **G 29** (2003) 2311 [`hep-ph/0306037`].

[76] BABAR collaboration, B. Aubert et al., *Search for the rare leptonic decay* $B^- \to \tau^-\bar\nu_\tau$, *Phys. Rev. Lett.* **95** (2005) 041804 [`hep-ex/0407038`].

[77] P. Chang, *Rare decays & new physics*, talk at *ICHEP* 2008, Philadelphia U.S.A. July 29 – August 5 2008.

[78] HPQCD collaboration, A. Gray et al., *The B meson decay constant from unquenched lattice QCD, Phys. Rev. Lett.* **95** (2005) 212001 [`hep-lat/0507015`].

[79] C. Bobeth, A.J. Buras and T. Ewerth, $\bar B \to X_s\ell^+\ell^-$ *in the MSSM at NNLO, Nucl. Phys.* **B 713** (2005) 522 [`hep-ph/0409293`].

[80] T. Huber, E. Lunghi, M. Misiak and D. Wyler, *Electromagnetic logarithms in* $\bar B \to X_s\ell^+\ell^-$, *Nucl. Phys.* **B 740** (2006) 105 [`hep-ph/0512066`].

[81] FlaviaNet Working Group on Kaon Decays collaboration, M. Antonelli et al., *Precision tests of the Standard Model with leptonic and semileptonic kaon decays*, `arXiv:0801.1817`.

[82] A.J. Buras, P. Gambino, M. Gorbahn, S. Jager and L. Silvestrini, ϵ'/ϵ *and rare K and B decays in the MSSM, Nucl. Phys.* **B 592** (2001) 55 [`hep-ph/0007313`].

[83] The E949 collaboration, A.V. Artamonov et al., *New measurement of the* $K^+ \to \pi^+, \nu, \bar\nu$ *branching ratio*, `arXiv:0808.2459`.

[84] UTfit collaboration, M. Bona et al., *Model-independent constraints on* $\Delta F = 2$ *operators and the scale of new physics, JHEP* **03** (2008) 049 [`arXiv:0707.0636`].

[85] T. Becher and M. Neubert, *Analysis of* $Br(B \to X_s\gamma)$ *at NNLO with a cut on photon energy, Phys. Rev. Lett.* **98** (2007) 022003 [`hep-ph/0610067`].

[86] P. Gambino and P. Giordano, *Normalizing inclusive rare B decays*, `arXiv:0805.0271`.

[87] Z. Ligeti, I.W. Stewart and F.J. Tackmann, *Treating the b quark distribution function with reliable uncertainties*, `arXiv:0807.1926`.

[88] M. Misiak, *QCD calculations of radiative B decays*, `arXiv:0808.3134`.

[89] P. Gambino, U. Haisch and M. Misiak, *Determining the sign of the $b \to s\gamma$ amplitude*, *Phys. Rev. Lett.* **94** (2005) 061803 [`hep-ph/0410155`].

[90] T. Hurth, G. Isidori, J.F. Kamenik and F. Mescia, *Constraints on new physics in MFV models: a model-independent analysis of $\Delta F = 1$ processes*, `arXiv:0807.5039`.

[91] C. Bobeth, M. Misiak and J. Urban, *Matching conditions for $b \to s\gamma$ and $b \to s$ gluon in extensions of the standard model*, *Nucl. Phys.* **B 567** (2000) 153 [`hep-ph/9904413`].

[92] G. Degrassi, P. Gambino and P. Slavich, *SusyBSG: a fortran code for $BR[B \to X_s\gamma]$ in the MSSM with minimal flavor violation*, `arXiv:0712.3265`.

[93] F. Mahmoudi, *SuperIso: a program for calculating the isospin asymmetry of $B \to K^*\gamma$ in the MSSM*, *Comput. Phys. Commun.* **178** (2008) 745 [`arXiv:0710.2067`]; *SuperIso v2.3: a program for calculating flavor physics observables in supersymmetry*, `arXiv:0808.3144`.

[94] J.R. Ellis, S. Heinemeyer, K.A. Olive and G. Weiglein, *Observability of the lightest CMSSM Higgs boson at hadron colliders*, *Phys. Lett.* **B 515** (2001) 348 [`hep-ph/0105061`].

[95] S. Ambrosanio, A. Dedes, S. Heinemeyer, S. Su and G. Weiglein, *Implications of the Higgs boson searches on different soft SUSY-breaking scenarios*, *Nucl. Phys.* **B 624** (2002) 3 [`hep-ph/0106255`].

[96] B.C. Allanach, *SOFTSUSY: a C++ program for calculating supersymmetric spectra*, *Comput. Phys. Commun.* **143** (2002) 305 [`hep-ph/0104145`].

[97] P. Gondolo, J. Edsjo, P. Ullio, L. Bergstrom, M. Schelke and E.A. Baltz, *DarkSUSY 4.00 neutralino dark matter made easy*, *New Astron. Rev.* **49** (2005) 149.

[98] P. Gondolo et al., *DarkSUSY: computing supersymmetric dark matter properties numerically*, *JCAP* **07** (2004) 008 [`astro-ph/0406204`].

[99] P. Skands et al., *SUSY Les Houches accord: interfacing SUSY spectrum calculators, decay packages and event generators*, *JHEP* **07** (2004) 036 [`hep-ph/0311123`].

[100] F. James and M. Roos, *Minuit: a system for function minimization and analysis of the parameter errors and correlations*, *Comput. Phys. Commun.* **10** (1975) 343.

[101] ATLAS collaboration, *Detector and physics performance technical design report 2*, CERN-LHCC-99-15 see
http://atlasinfo.cern.ch/Atlas/GROUPS/PHYSICS/TDR/access.html
https://twiki.cern.ch/twiki/bin/view/Atlas/SUSYWorkingGroup.

[102] CMS collaboration, G.L. Bayatian et al., *CMS technical design report, volume II: physics performance*, *J. Phys.* **G 34** (2007) 995 [CERN-LHCC-2006-021] [CMS-TDR-008-2] see
http://cmsdoc.cern.ch/cms/cpt/tdr/.

[103] J.-J. Blaising, A. De Roeck, J. Ellis, F. Gianotti, P. Janot, G. Rolandi and D. Schlatter, *Potential LHC contributions to Europe's future strategy at the high energy frontier*;
J.R. Ellis, *Physics at LHC*, *Acta Phys. Polon.* **B38** (2007) 1071 [`hep-ph/0611237`].

[104] B.C. Allanach et al., *The snowmass points and slopes: benchmarks for SUSY searches*, *Eur. Phys. J.* **C 25** (2002) 113 [*eConf* **C010630** (2001) P125] [`hep-ph/0202233`].

[105] M. Battaglia et al., *Proposed post-LEP benchmarks for supersymmetry*, *Eur. Phys. J.* **C 22** (2001) 535 [`hep-ph/0106204`].

[106] M. Battaglia et al., *Updated post-WMAP benchmarks for supersymmetry*, Eur. Phys. J. **C 33** (2004) 273 [`hep-ph/0306219`].

[107] LHC/LC STUDY GROUP collaboration, G. Weiglein et al., *Physics interplay of the LHC and the ILC*, Phys. Rept. **426** (2006) 47 [`hep-ph/0410364`].

[108] T. Plehn, *PROSPINO2*, http://www.ph.ed.ac.uk/∼tplehn/prospino/.

[109] D0 collaboration, V.M. Abazov et al., *Search for squarks and gluinos in events with jets and missing transverse energy using* $2.1\,fb^{-1}$ *of* $p\bar{p}$ *collision data at* $\sqrt{s} = 1.96\,TeV$, Phys. Lett. **B 660** (2008) 449 [`arXiv:0712.3805`].

[110] CDF collaboration, S. Dube et al., *Unified search for associated production of chargino-neutralino using leptons*, CDF public note 9176, http://www-cdf.fnal.gov/physics/exotic/r2a/20080110.trilepton_dube.

[111] M.M. Nojiri, G. Polesello and D.R. Tovey, *Constraining dark matter in the MSSM at the LHC*, JHEP **03** (2006) 063 [`hep-ph/0512204`].

[112] E.A. Baltz, M. Battaglia, M.E. Peskin and T. Wizansky, *Determination of dark matter properties at high-energy colliders*, Phys. Rev. **D 74** (2006) 103521 [`hep-ph/0602187`].

[113] H. Baer, A. Mustafayev, S. Profumo, A. Belyaev and X. Tata, *Neutralino cold dark matter in a one parameter extension of the minimal supergravity model*, Phys. Rev. **D 71** (2005) 095008 [`hep-ph/0412059`].

[114] H. Baer, A. Mustafayev, S. Profumo, A. Belyaev and X. Tata, *Direct, indirect and collider detection of neutralino dark matter in SUSY models with non-universal Higgs masses*, JHEP **07** (2005) 065 [`hep-ph/0504001`].

[115] J. Ellis, K.A. Olive and P. Sandick, *Varying the universality of supersymmetry-breaking contributions to MSSM Higgs boson masses*, `arXiv:0805.2343`.